

## Supporting Information for

### Inhalable Viromimetic Polymer Nanoparticle Vaccine (iVPNVax) in a Subcutaneous-prime/inhalation-boost Vaccination Schedule for Eliciting Durable Mucosal and Systemic Immune Protection

Zhenyi Zhu<sup>1,2</sup>, Xinyu Zhuang<sup>3</sup>, Zichao Huang<sup>1,2</sup>, Chenchao Zhang<sup>3,4</sup>, Tong Zhang<sup>3,4</sup>,  
Liping Liu<sup>1,2</sup>, Aolin Sun<sup>1,2</sup>, Jiangai Long<sup>1,2</sup>, Yusong Cao<sup>1,2</sup>, Yaxin Zhang<sup>1,2</sup>, Ying  
Xing<sup>1,2</sup>, Songhui Yang<sup>3</sup>, Jianan Peng<sup>3</sup>, Siyou Huang<sup>3</sup>, Ningning Hu<sup>3</sup>, Mingyao Tian<sup>3\*</sup>,  
Wantong Song<sup>1,2,5\*</sup>, Xuesi Chen<sup>1,2,5\*</sup>

Correspondence to: [wtsong@ciac.ac.cn](mailto:wtsong@ciac.ac.cn) (W. Song)

## **This PDF file includes:**

### **Materials and Methods**

#### **Figures S1 to S13**

#### **Tables S1 to S4**

## **Experimental Section**

### **Materials**

D- and L-lactide monomers were generously provided by Changchun SinoBiomaterials Co., Ltd. The RBD protein of the SARS-CoV-2 Omicron BA.1 strain (Omicron CoV/human/CHN\_CVRI-01/2022), BA.2 (Omicron CoV/human/CHN\_CVRI-04/2022) and Imject Alum adjuvant were kindly supplied by the Changchun Veterinary Research Institute. Anhydrous methylbenzene was prepared via vacuum distillation. Maleimide-PEG-hydroxyl (5 kDa) was sourced from Beijing JenKem Technology Co., Ltd. Anhydrous ethyl acetate was purchased from Beijing Energy Chemical Co., Ltd. Tin(II) 2-ethylhexanoate, 2-iminothiolane hydrochloride, and L-cysteine hydrochloride monohydrate were obtained from Shanghai Aladdin Biochemical Technology Co., Ltd. IMDQ (CAS: 1258457-59-8) was purchased from Suzhou Nuobeike Biotechnology Co., Ltd. Ovalbumin (OVA, Cat. A5503) was purchased from Sigma-Aldrich. Sulfo-Cy5-succinimidyl ester (Cy5-NHS) was purchased from Meilun Biotechnology Co., Ltd., used for OVA protein labeling, and purified using a 10 kDa ultrafiltration device. Bovine serum albumin V (BSA, Cat. A8020) was purchased from Beijing Solarbio Science & Technology Co., Ltd. Goat anti-mouse IgG (H+L) secondary antibody, HRP (Cat. 31430), and the BCA Protein Assay Kit (Cat. 23225) were from Thermo Fisher Scientific. Goat anti-mouse IgG1 (HRP) (Cat. ab97240), goat anti-mouse IgG2c heavy chain (HRP) (Cat. ab97255) and goat anti-mouse IgA alpha chain (HRP) (Cat. ab97235) were from Abcam (Shanghai) Trading Co., Ltd. 3,3',5,5'-Tetramethylbenzidine (TMB, Cat. P0209) and Antifade Mounting Medium with DAPI (Cat. P0131) were from Shanghai Beyotime Biotechnology Co., Ltd. The ultrafiltration device with a 10 kDa MWCO was the Amicon Ultra-0.5 Centrifugal Filter Unit (Cat. UFC5010) from Millipore Sigma Co., Ltd., and the 300 kDa MWCO device was the Vivaspin® 500 Centrifugal Concentrator (Cat. VS0152) from Sartorius Co., Ltd. The cell activation cocktail (with Brefeldin A) (Cat. 423303) and intracellular staining permeabilization wash buffer (Cat. 421002) were purchased from BioLegend. UNIQ-10 Column Trizol Total RNA Isolation Kit was purchased from Sangon Biotech, Shanghai. HiScript II U + One Step qRT-PCR Probe Kit was purchase from Vazyme, China. Other reagents and solvents were obtained from Sinopharm Chemical Reagent Co., Ltd.

### **Animals**

All animal experiments in this study were approved by the Institutional Animal Care and Use Committee (IACUC) of the Institute of Medical Experimental Animals, Chinese Academy of Medical Sciences, with approval number IACUC of AMMS-11-2024-049. Female C57BL/6 mice (6-8 weeks) and male LVG hamsters (3-4 weeks) were obtained from Beijing Vital River Laboratory Animal Technology Co., Ltd. (Beijing, China).

Synthesis and Characterization of Maleimide-Terminated Polyethylene Glycol-Block-Poly (D, L-

### Lactic Acid) Copolymer (MalPEG-*b*-PLA)

MalPEG-*b*-PLA was prepared via ring-opening polymerization of D, L-lactide initiated by hydroxyl-terminated MalPEG<sub>5k</sub>. D- and L-lactide (10 g each) were recrystallized from anhydrous ethyl acetate (>3 times) at 90°C, followed by vacuum drying to yield purified monomers. In a glove box, purified D, L-lactide (7 g, 48.6 mmol) and MalPEG<sub>5k</sub>-OH (1 g, 0.2 mmol) were dissolved in anhydrous toluene (15 mL), and Sn(Oct)<sub>2</sub> (15 mg, resolved in 10 mL toluene) was added under nitrogen. The reaction mixture was sealed and stirred at 110°C for 24 h, then precipitated into cold ether, collected, and reprecipitated from dichloromethane 2-3 times. After vacuum drying, a slightly yellowish-white MalPEG-*b*-PLA solid was obtained. Polymer structure was confirmed by <sup>1</sup>H NMR (DMSO-*d*<sub>6</sub>).

### Synthesis and Characterization of IMDQ-PEG-*b*-PLA

IMDQ-PEG-*b*-PLA was obtained by coupling IMDQ (9.4 mg, 27.0 nmol) with MalPEG-*b*-PLA (500 mg, 13.5 nmol) in 5 mL dimethyl sulfoxide containing 5% triethylamine. The reaction was performed at room temperature for 72 h under sealed conditions. The crude product was dialyzed against deionized water and lyophilized to remove excess IMDQ, yielding a pale-yellow solid. Structure confirmation was performed by <sup>1</sup>H NMR (DMSO-*d*<sub>6</sub>).

### Preparation of VPNVax and iVPNVax Nanoparticles

VPNVax and iVPNVax nanoparticles were prepared using a microfluidic method. For the organic phase (OP), Mal-PEG-*b*-PLA and IMDQ-PEG-*b*-PLA were mixed at a mass ratio of 1:19 (subcutaneous injection) or 1:4 (for inhalation injection) and dissolved in acetone at a total polymer concentration of 10 mg/mL. Ultrapure water was used as the aqueous phase (AP). The OP and AP solutions were separately loaded into glass syringes and injected into a microfluidic mixing chip for rapid mixing. The total flow rate (TFR) was set to 6 mL/min with an organic-to-aqueous flow-rate ratio (FRR) of 1:5. The resulting nanoparticle suspension was collected immediately at the outlet. The collected suspension was transferred into a dialysis bag (molecular weight cutoff: 3.5 kDa) and dialyzed against ultrapure water for at least 4 h to remove the organic solvent and exchange the buffer, yielding iVPNVax nanoparticles. VPNVax nanoparticles were prepared under identical microfluidic conditions, except that the organic phase consisted solely of Mal-PEG-*b*-PLA dissolved in acetone at a concentration of 10 mg/mL. After dialysis, all nanoparticle suspensions were sterile-filtered through a 0.22 μm membrane and stored at 4°C prior to further characterization and use. The particle size, polydispersity index (PDI), and zeta potential of the nanoparticles were measured using Zetasizer Nano ZS (Malvern analytical Co. Ltd).

### Antigen Thiolation and Purification

Antigen proteins were thiolated using Traut's reagent prior to nanoparticle conjugation. For OVA, 180 μg protein was dissolved in deionized water (10 mg/mL), adjusted to pH 8.0-8.5 with 10 μL PB buffer, and reacted with 5.0 μg Traut's reagent (2 μg/μL in PB) for 1 h at room temperature. The product was purified by ultrafiltration (MWCO 10 kDa) with deionized water, concentrated to 1.8 μg/μL, and quantified by BCA assay (Thermo Fisher Scientific). BA.1 antigens were modified using the same procedure.

### VPNVax-OVA and iVPNVax-OVA Preparation

Thiolated antigens were conjugated to MalPEG-*b*-PLA/IMDQ-PEG-*b*-PLA nanoparticles via maleimide-thiol click chemistry reaction to prepare iVPNVax-OVA. For example, 2 µg of thiolated OVA was added to 1 mg of nanoparticles, incubated overnight at 4°C with gentle shaking, and purified by repeated ultrafiltration (MWCO 300 kDa). Residual maleimide groups were quenched with cysteine. VPNVax-OVA was prepared using the same formulation using VPNVax nanoparticles.

For subcutaneous administration, VPNVax-OVA or iVPNVax-OVA was adjusted to a final concentration of 5 mg (corresponding to 10 µg antigen protein) per 100 µL per dose (IMDQ-polymer molar ratio of 5%); for inhalation administration, and VPNVax-OVA /iVPNVax-OVA was adjusted to 1.25 mg (corresponding to 2.5 µg antigen protein) per 75 µL per dose (IMDQ-polymer molar ratio of 20%).

For fluorescent tracking studies, VPNVax-OVA/Cy5 and iVPNVax-OVA/Cy5 were prepared using the same procedure. Briefly, OVA was pre-labeled with Cy5-NHS, followed by dialysis using a 3.5 kDa molecular weight cutoff membrane to remove unreacted Cy5-NHS. The purified OVA/Cy5 was lyophilized and subsequently thiolated following the same protocol as unlabeled OVA before being used for the preparation of VPNVax-OVA/Cy5 and iVPNVax-OVA/Cy5 nanoparticles. Conjugated antigen content was determined by BCA assay, and droplet morphology was examined by a confocal laser scanning microscope (CLSM, Carl Zeiss LSM 700, Germany). The particle size and polydispersity index (PDI) of the nanovaccines were measured using Zetasizer Nano ZS (Malvern analytical Co. Ltd).

#### Animal Immunization

Specifically, 6-8 weeks old C57BL/6 mice were randomly assigned to groups and immunized either by subcutaneous injection at the tail base with vaccine formulations or controls, or via aerosol inhalation using a tracheal delivery device following intraperitoneal anesthesia. For OVA and BA.1 antigens, the immunization dose was 10 µg protein per mouse per injection. In aluminum-adjuvanted formulations, 300 µg alum (10 µL) was added dropwise to the vaccine solution and thoroughly mixed prior to administration.

Mice were anesthetized with tribromoethanol and placed in a supine position on an intubation platform. The trachea was exposed and visualized under illumination. A microsyringe equipped with a microsyringer (Liquid PenWu Device, BioJane, China) was gently inserted into the trachea. A defined volume of vaccine formulation (e.g., 70 µL) was administered directly into the airway to achieve intratracheal delivery. After administration, mice were kept in an upright position for a short period to facilitate distribution of the formulation in the lungs.

#### Histology, Immunofluorescence, and Imaging

For the pulmonary accumulation and retention study following inhalation, OVA was labeled with Cy5 (OVA/Cy5) and formulated into VPNVax or iVPNVax. Mice were anesthetized intraperitoneally and administered 10 µg OVA per mouse via aerosolization using a tracheal delivery device. The OVA control group received the same dose of soluble OVA/Cy5 + IMDQ. Lungs were collected on days 1, 3, and 7 post-immunization for fluorescence imaging, and mean fluorescence intensity was quantified using ImageJ. On day 14, lungs were harvested, dehydrated through graded alcohols, sectioned, and imaged with an Olympus slide scanning system.

For GC activation analysis, mediastinal lymph nodes were collected on day 42 post-immunization

for frozen section preparation. Sections were stained with Alexa Fluor 594-conjugated anti-B220 (B cell follicles) and Alexa Fluor 488-conjugated anti-GL7 (GC B cells) antibodies (1:100). Imaging was performed with a Zeiss LSM 700 confocal microscope, and GC formation was determined based on the colocalization of B220 and GL7 signals.

#### Flow Cytometric Analysis of Pulmonary Vaccine Uptake

Mice were anesthetized intraperitoneally and administered soluble OVA/Cy5 + IMDQ, VPNVax-OVA/Cy5, or iVPNVax-OVA/Cy5 (10 µg OVA per mouse) via aerosolization using a tracheal delivery device. At 24 h post-administration, lungs were harvested and processed into single-cell suspensions. Cells were stained with a cocktail of antibodies, including anti-CD45, anti-CD11c, anti-CD19, anti-CD3, anti-F4/80, and anti-CD11b, followed by flow cytometric analysis (BD FACS Celesta).

#### FACS Analysis of Pulmonary APC Activation

Mice were anesthetized intraperitoneally and administered soluble OVA/Cy5 + IMDQ, VPNVax-OVA/Cy5 or iVPNVax-OVA/Cy5 (10 µg OVA per mouse) via aerosolization using a tracheal delivery device. Lungs were collected 48 h post-administration and processed into single-cell suspensions. Cells were stained with a panel of antibodies, including anti-CD45, anti-CD11c, anti-CD19, anti-F4/80, anti-CD11b, anti-CD86, and anti-MHC II, followed by flow cytometric analysis.

#### Blood Collection and Serum Preparation

Approximately 500 µL of blood was collected from the retro-orbital venous plexus of mice into 1.5 mL tubes without anticoagulant. Samples were incubated at 37°C for 30 min, followed by centrifugation at 900 × g for 15 min. The supernatant serum was collected for immediate analysis or aliquoted and stored at -80°C until use, avoiding repeated freeze-thaw cycles.

#### BALF Collection

At designated time points, mice were anesthetized, placed in a supine position, and the trachea was exposed. The trachea was incised with sterile scissors, and a trimmed 1 mL syringe needle was inserted approximately 5 mm below the larynx and secured with suture. One milliliter of sterile PBS (pH 7.4) was gently instilled into the lungs and then withdrawn to collect the lavage fluid. This procedure was repeated 2-3 times to maximize recovery. Collected BALF was centrifuged at 500 × g for 10 min at 4°C to remove cells and debris. Supernatants were used immediately for analysis or aliquoted and stored at -80°C, avoiding repeated freeze-thaw cycles.

#### Antigen-Specific Antibody Titer Measurement

Antibody titers were measured by enzyme-linked immunosorbent assay (ELISA). Antigen proteins (10 µg/mL in PBS, 100 µL/well) were coated onto 96-well plates and incubated overnight at 4°C. Plates were washed and blocked with 2% BSA in PBS (200 µL/well) for 2 h at room temperature. Mouse serum or BALF was serially 4-fold diluted from the stock and added to the wells, followed by 2 h incubation at room temperature. After washing, HRP-conjugated goat anti-mouse secondary antibodies against IgG, IgG1, IgG2c, or IgA(1:5000) were applied for 1 h. Color development was performed with TMB for 15 min, stopped with 2 N H<sub>2</sub>SO<sub>4</sub>, and absorbance was recorded at 450 nm. The titer was defined as the highest dilution giving an OD above the cutoff (blank + 0.03), with

cutoffs adjusted as needed for controls.

#### Analysis of Immune Cells in Spleen and Mediastinal Lymph Nodes

Mice were subcutaneously immunized on days 0 and 14 with OVA + Alum or iVPNVax (10 µg OVA per mouse). On day 28, mice were anesthetized intraperitoneally and administered OVA + IMDQ, VPNVax-OVA, or iVPNVax-OVA (10 µg OVA per mouse) via a tracheal delivery device. On day 42, spleens and mediastinal lymph nodes (mLN) were collected. Spleens were processed into single-cell suspensions following red blood cell lysis. A portion of splenocytes was used for IFN $\gamma$  ELISpot according to the manufacturer's protocol. The remaining splenocytes were stained with antibody panels for total DCs (CD11c<sup>+</sup>), cDC1 (CD11c<sup>+</sup>CD103<sup>+</sup>CD11b<sup>-</sup>), cDC2 (CD11c<sup>+</sup>CD103<sup>-</sup>CD11b<sup>+</sup>), pDC (CD11c<sup>-</sup>CD11b<sup>+</sup>SiglecH<sup>+</sup>), and DC activation markers (CD80, CD86, MHC II). Additional staining with anti-CD4, anti-CD8, anti-CXCR5, anti-PD-1, anti-CD19, anti-CD44, and anti-CD138 was performed to analyze the proportions and activation states of CD4 T cells, CD8 T cells, Tfh cells, and plasma blasts.

mLN samples were processed in the same manner as spleens and analyzed by flow cytometry with dimensionality reduction (t-SNE/UMAP) to assess DC activation.

#### Pulmonary Memory T Cell Analysis

At designated time points post-immunization, lungs were collected and processed into single-cell suspensions. Cells were stained with anti-CD4, anti-CD8, anti-CD44, anti-CD69, and anti-CD103 to evaluate memory CD4<sup>+</sup> T cells, memory CD8<sup>+</sup> T cells, and CD8<sup>+</sup> T<sub>RM</sub>. For functional T<sub>RM</sub> analysis, cells were stimulated with antigen for 5 h in the presence of Brefeldin A, followed by intracellular staining for IFN $\gamma$  and IL-17A (IFN $\gamma$ <sup>+</sup>/IL-17A<sup>+</sup>).

All samples were fixed with 4% paraformaldehyde, acquired on a BD FACS Celesta flow cytometer, and analyzed using FlowJo 10 software.

#### Authentic SARS-CoV-2 Neutralization Assay

Live virus neutralization assays were conducted in the biosafety level 3 (BSL-3) laboratory. Neutralizing antibody titers were determined using a microneutralization assay. Heat-inactivated sera (56°C, 30 min) were serially diluted (1:20-1:20480) and mixed (1:1) with 100 × TCID<sub>50</sub> SARS-CoV-2 Omicron BA.1 (Omicron CoV/human/CHN\_CVRI-01/2022) or BA.2 (Omicron CoV/human/CHN\_CVRI-04/2022). After 1 h incubation at 37°C, 5 × 10<sup>3</sup> Vero E6 cells (100 µL) were added. Cytopathic effect was evaluated on day 5 post-infection, and titers were calculated via the Reed-Muench method.

#### Protective Efficacy in Mice

On day 14 after booster immunization, mice were anesthetized and intranasally challenged with 5 × 10<sup>3</sup> TCID<sub>50</sub> of SARS-CoV-2 Omicron BA.1 in a BSL-3 facility. Body weight and survival were monitored daily. Throat swabs were collected on days 3 and 5 post-infection for viral load analysis. Nasal turbinates, trachea, and lungs were harvested for qPCR quantification of N and E genes, as well as histopathology to assess lung injury.

#### Quantitative PCR (qPCR)

RNA from throat swabs, nasal turbinates, trachea, and lungs was extracted using the UNIQ-10

Column Trizol Total RNA Isolation Kit (Sangon Biotech, Shanghai). Viral load was determined with the HiScript II U + One Step qRT-PCR Probe Kit (Vazyme, China) following the manufacturer's instructions. Primer and probe sequences are listed in **Table S3**.

#### Statistical Analysis

All experiments were repeated independently at least three times. Data are presented as mean  $\pm$  SD. Two-tailed unpaired Student's t-tests were used for pairwise comparisons, while one-way ANOVA with Bonferroni post hoc tests was applied for multiple-group analyses. Two-way ANOVA with Tukey's multiple comparisons was used where appropriate. "ns" indicates no significant difference.

## Supplemental Figures and Tables

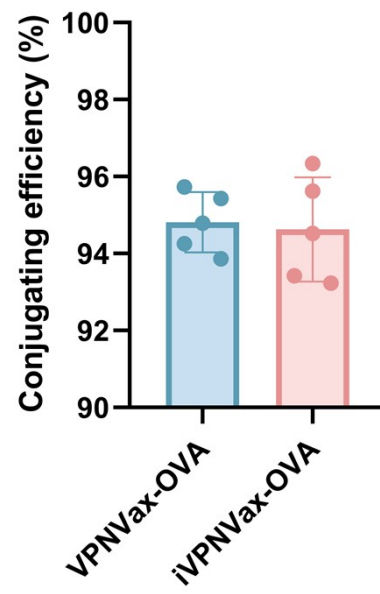


**Figure S1.** Antigen conjugating efficiency of VPNVax-OVA and iVPNVax-OVA.  $n = 5$ .

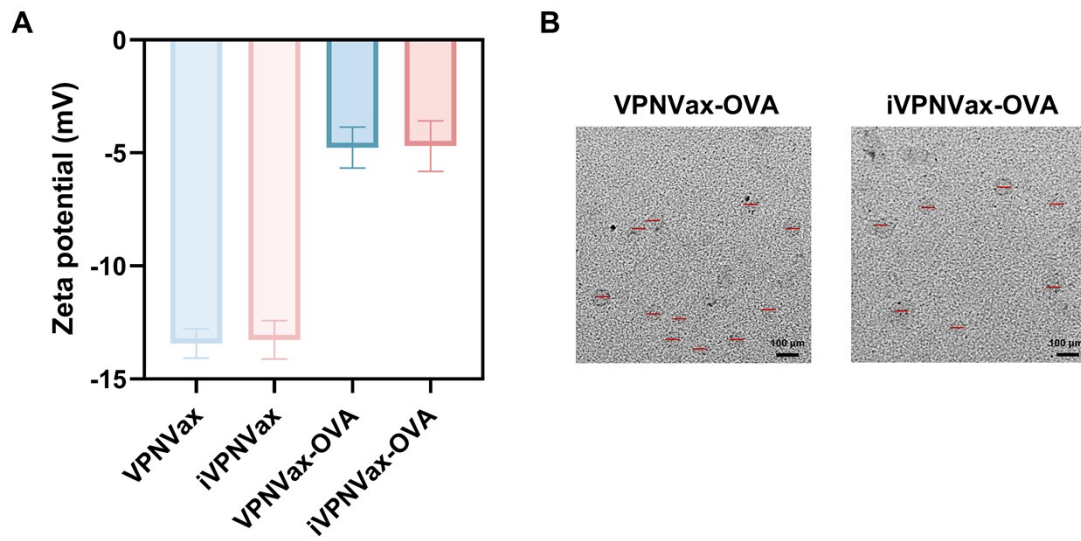


**Figure S2.** A) Characterization of the zeta potential of VPNVax, iVPNVax, VPNVax-OVA and iVPNVax-OVA nanoparticles.  $n = 5$ . B) Representative TEM images of VPNVax-OVA and iVPNVax-OVA nanoparticles.

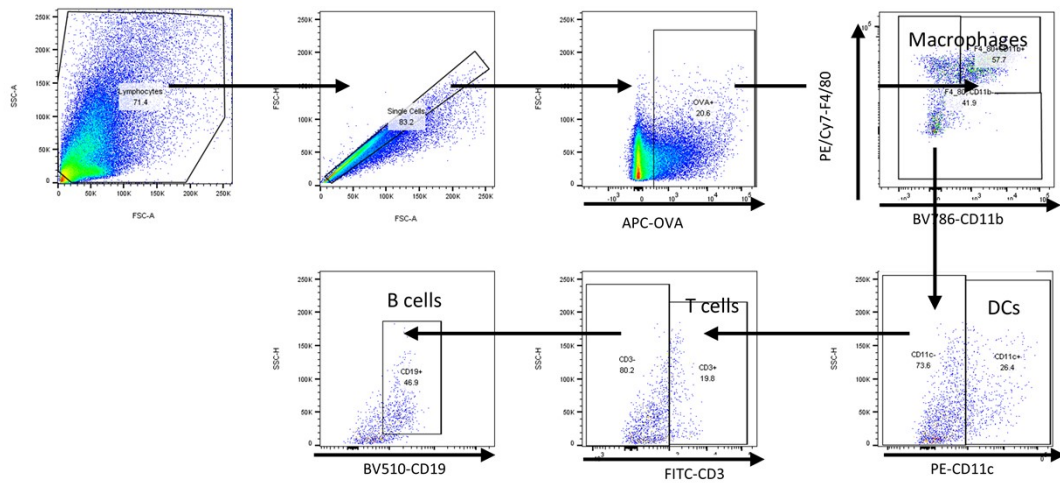


**Figure S3.** Gating strategy showing the distribution of Cy5-labeled vaccines in various pulmonary immune cells (T cells, B cells, DCs, and macrophages) 24 h after inhalation treatment.

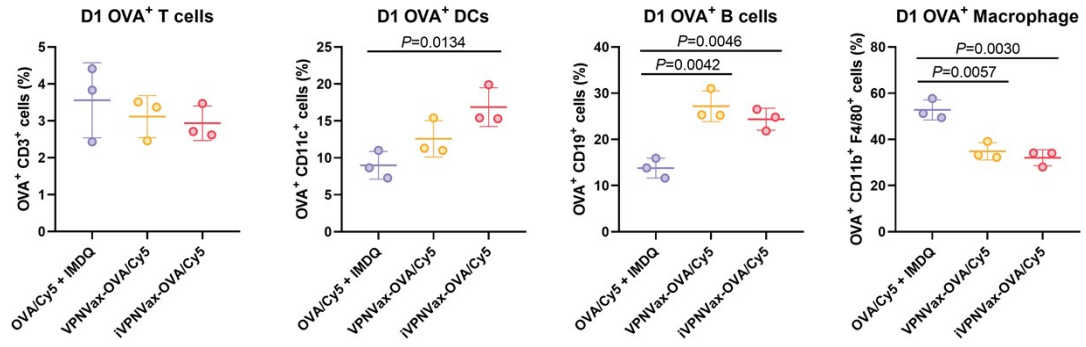


**Figure S4.** Proportions of Cy5-labeled vaccine uptake among various pulmonary immune cells (T cells, B cells, DCs, and macrophages) 24 h after inhalation treatment.  $n = 3$ .

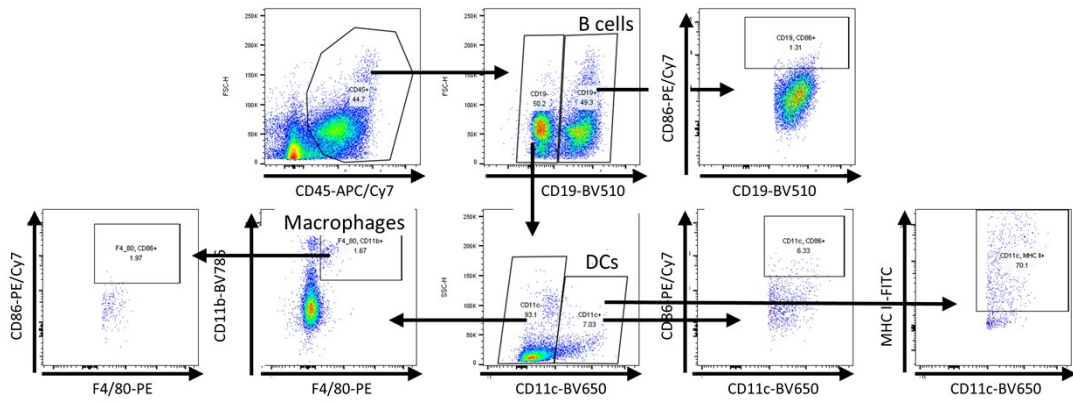


**Figure S5.** Gating strategies for immune cell infiltration and activation of pulmonary APCs (B cells, DCs, and macrophages) assessed by CD86 and MHCII expression in mouse lungs 48 h after inhalation treatment.

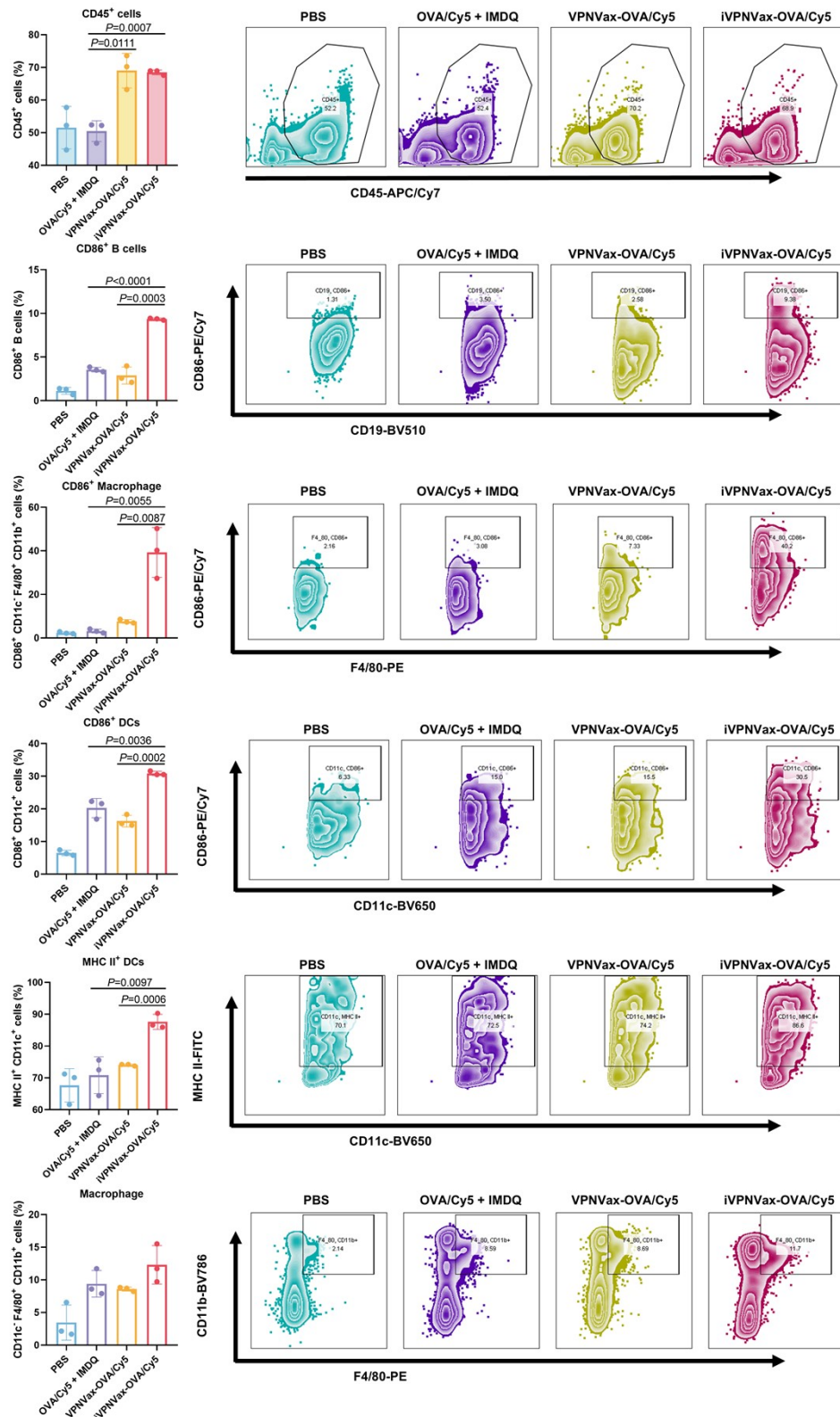


**Figure S6.** Representative plots of immune cell infiltration and activation of pulmonary APCs (B cells, DCs, and macrophages), assessed by CD86 and MHCII expression, in mouse lungs 48 h after inhalation treatment.  $n = 3$ .

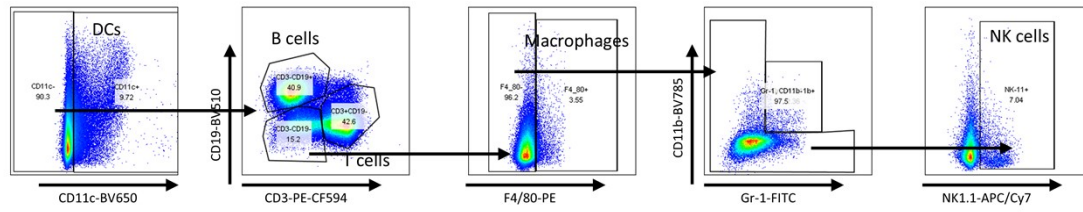


**Figure S7.** Gating strategy for tNSE dimensionality reduction analysis of C57BL/6 mice on day 42 following two subcutaneous priming immunizations and an inhalation booster.

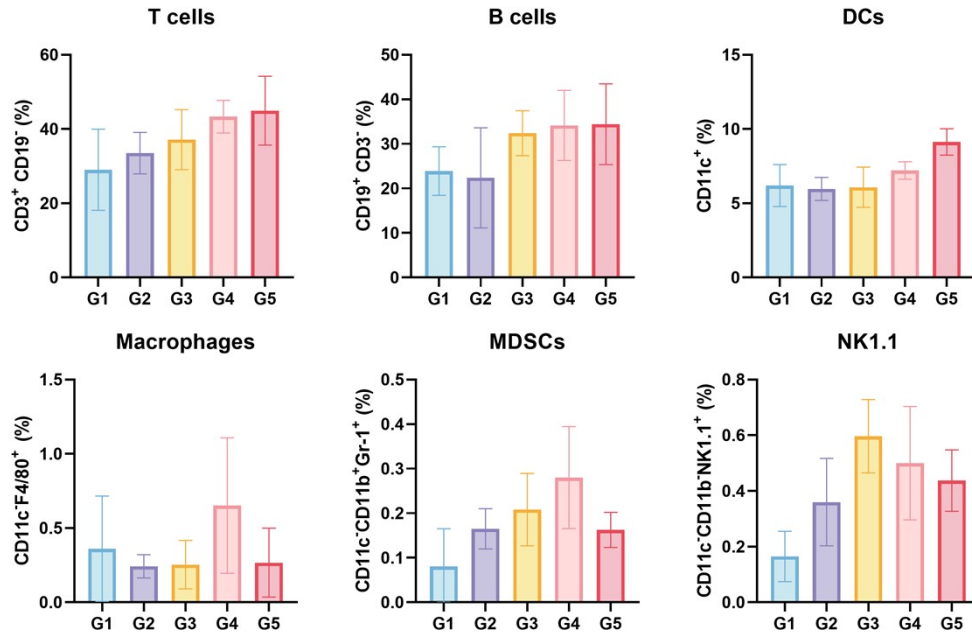


**Figure S8.** Infiltration proportions of different immune cells (T cells, B cells, DCs, Macrophages, MDSCs, and NK1.1<sup>+</sup> cells) in mouse mLNs on day 42 following two subcutaneous priming immunizations and an inhalation booster. G1: PBS (s.c.) + PBS (inh.), G2: OVA + Alum (s.c.) + OVA + IMDQ (inh.), G3: OVA + Alum (s.c.) + VPNVax-OVA (inh.), G4: OVA + Alum (s.c.) + iVPNVax-OVA (inh.), G5: iVPNVax-OVA (s.c.) + iVPNVax-OVA (inh.).  $n = 6$ .

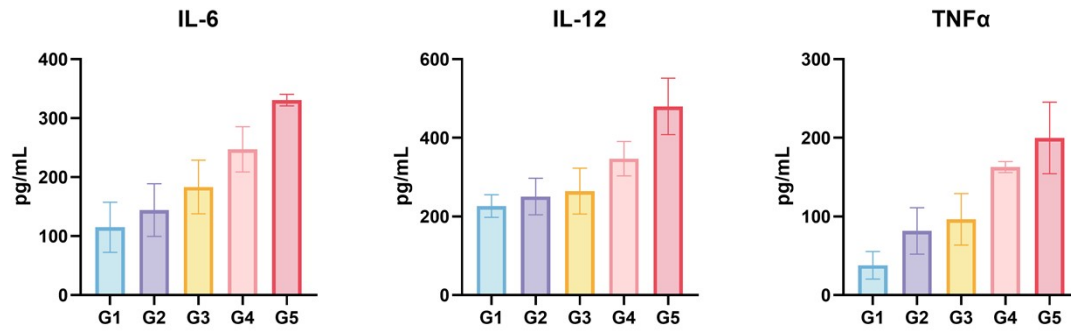


**Figure S9.** Cytokine analysis of IFN- $\gamma$ , IL-12, and IL-6 in mouse mLNs on day 42 following two subcutaneous priming immunizations and an inhalation booster. G1: PBS (s.c.) + PBS (inh.), G2: OVA + Alum (s.c.) + OVA + IMDQ (inh.), G3: OVA + Alum (s.c.) + VPNVax-OVA (inh.), G4: OVA + Alum (s.c.) + iVPNVax-OVA (inh.), G5: iVPNVax-OVA (s.c.) + iVPNVax-OVA (inh.).  $n = 6$ .

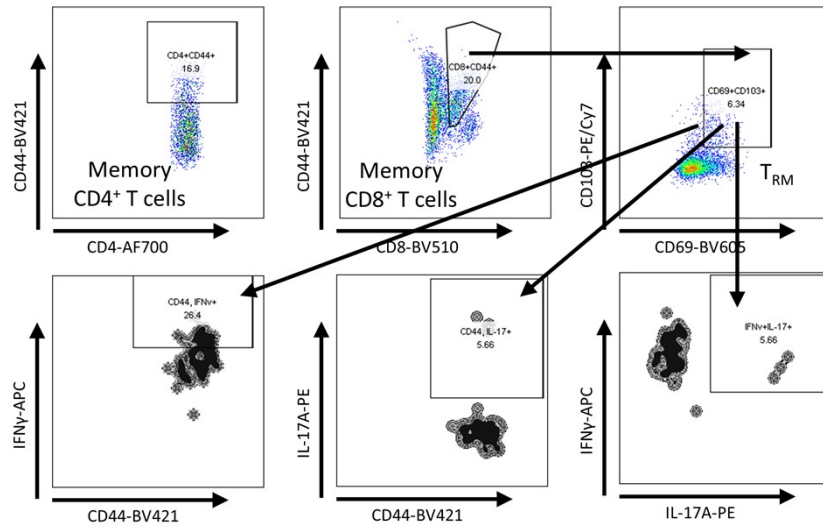


**Figure S10.** Gating strategies for memory T cells,  $T_{RM}$  and functional  $T_{RM}$  in mouse lungs on day 42 following two subcutaneous priming immunizations and an inhalation booster.

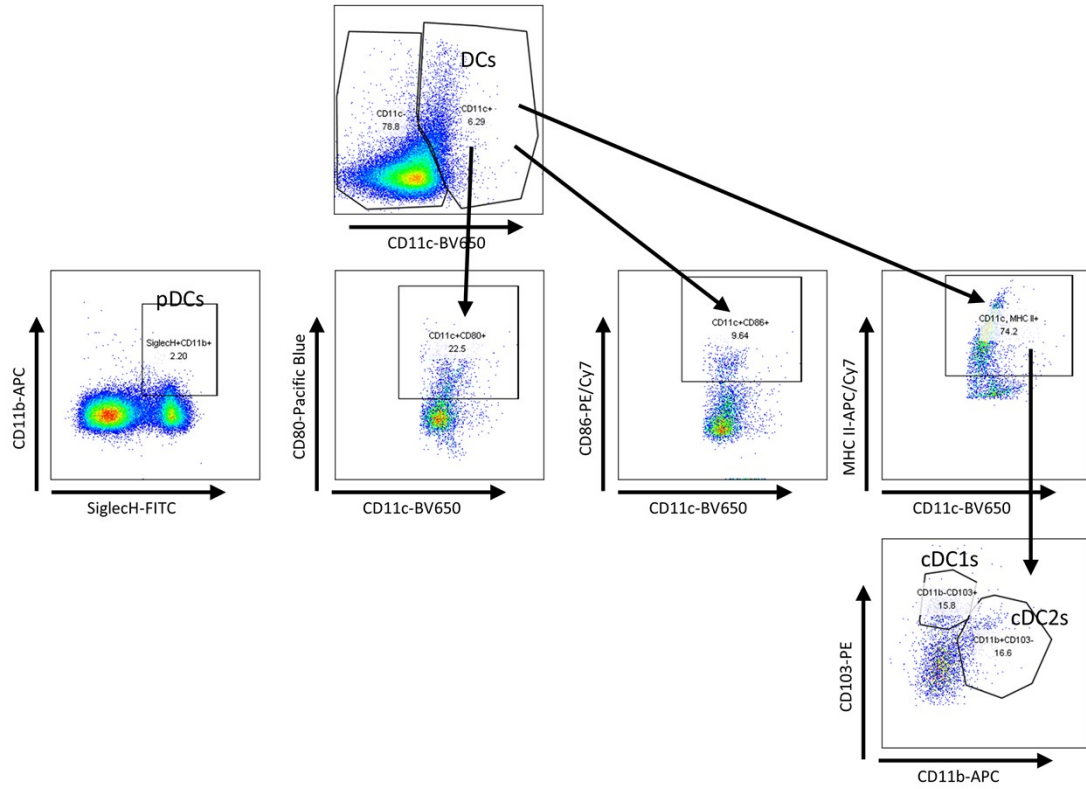


**Figure S11.** Gating strategies for DCs, including classical subsets (cDC1 and cDC2), plasmacytoid DCs (pDCs), and activated DCs (CD80<sup>+</sup>, CD86<sup>+</sup>, MHCII<sup>+</sup>) in mouse spleens on day 42 following two subcutaneous priming immunizations and an inhalation booster.

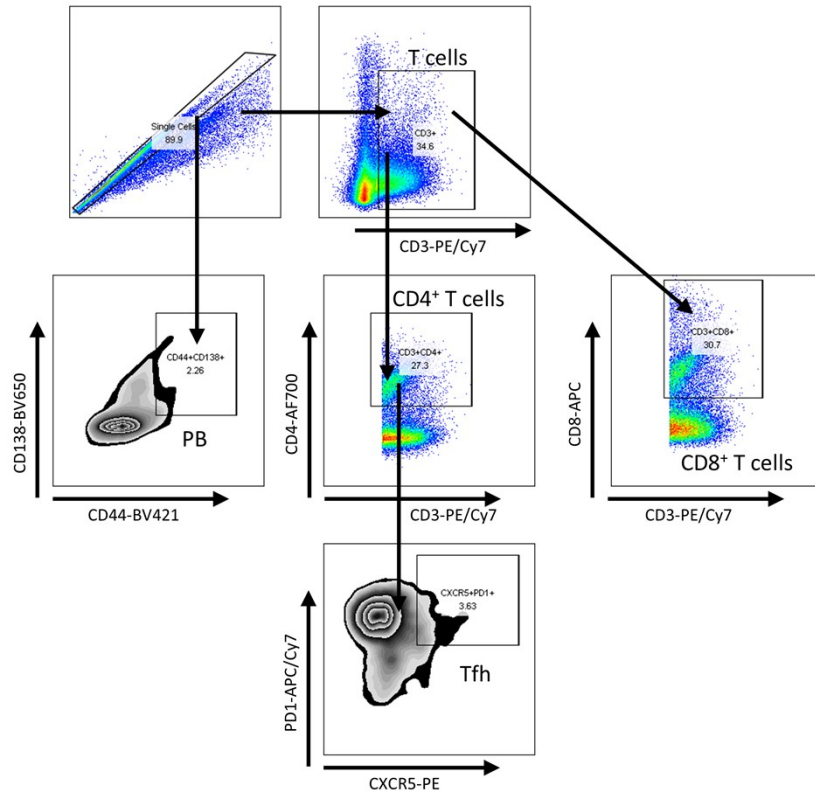


**Figure S12.** Gating strategies for CD4<sup>+</sup> T cells, CD8<sup>+</sup> T cells, Tfh and PB cells in mouse spleens on day 42 following two subcutaneous priming immunizations and an inhalation booster.

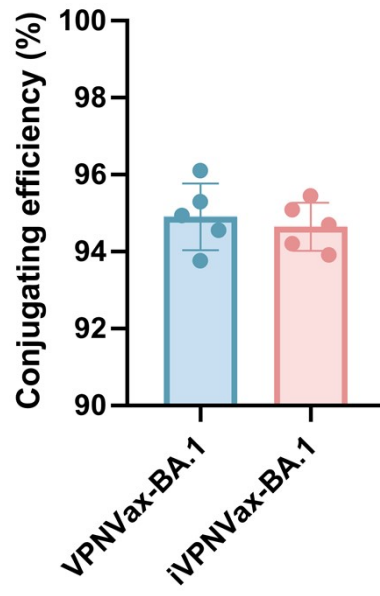


**Figure S13.** Antigen conjugating efficiency of VPNVax-BA.1 and iVPNVax- BA.1.  $n = 5$ .

**Table S1.** Evaluation criteria for lung damage in hamsters. The assessment includes alveolar wall thickening, inflammatory cell infiltration, hemorrhage, eosinophilic material exudation, necrosis of airway and alveolar cells, and perivascular edema.

**Four-level grading system**

<b>Level (Number)</b>	<b>Category</b>	<b>Description</b>
<b>0</b>	Within the normal range	Under research conditions, considering factors such as the animal's age, sex, and strain, the tissue is considered normal. Changes observed under other conditions may be considered abnormal.
<b>1</b>	Very slight	Changes observed slightly exceed the normal range.
<b>2</b>	Slight	Changes observed slightly exceed the normal range.
<b>3</b>	Moderate	The lesions are evident and are likely to become more severe.
<b>4</b>	Severe	The lesions are very serious (the lesions have affected the entire tissue or organ).

**Table S2** Histopathological features and corresponding arrow color annotations.

<b>Arrow Color</b>	<b>Pathological Feature</b>
Orange	Vascular congestion
Purple	Mild alveolar dilation
Red	Alveolar hemorrhage
Gray	Consolidation
Yellow	Lymphocyte exudation
Brown	Thickening of alveolar walls
Black	Irregular epithelial cell arrangement
Green	Lymphocyte infiltration
Blue	Granulocyte infiltration

**Table S3.** Antibodies used in the study.

<b>Antibodies</b>	<b>Company</b>	<b>Catalog No.</b>
PE anti-mouse CD11c	BioLegend	117308
BV650 anti-mouse CD11c	BioLegend	117339
FITC anti-mouse CD3	BioLegend	100204
PE-CF594 anti-mouse CD3	BioLegend	100245
PE/Cy7 anti-mouse CD3	BioLegend	100219
AF700 anti-mouse CD4	BioLegend	100536
APC anti-mouse CD8	BioLegend	100712
BV510 anti-mouse CD8	BioLegend	100751
BV510 anti-mouse CD19	BioLegend	115545
Pacific Blue anti-mouse CD80	BioLegend	104723
PE-Cy7 anti-mouse CD86	BioLegend	105013
FITC anti-mouse MHC II	BioLegend	107606
APC-Cy7 anti-mouse MHC II	BioLegend	116630
PE/Cy7 anti-mouse F4/80	BioLegend	123113
PE anti-mouse F4/80	BioLegend	111603
BV605 anti-mouse CD69	BioLegend	104529
APC anti-mouse IFN $\gamma$	BioLegend	505809
PE anti-mouse IL-17A	BioLegend	506903
PE-Cy7 anti-mouse CD103	BioLegend	121425
PE anti-mouse CD103	BioLegend	110903
FITC anti-mouse Gr-1	BioLegend	108405
APC/Cy7 anti-mouse NK-1.1	BioLegend	108723
APC/Cy7 anti-mouse CD45	BioLegend	103115
BV785 anti-mouse CD11b	BioLegend	101243
APC anti-mouse CD11b	BioLegend	101211
PE anti-mouse CXCR5	BioLegend	145503
APC-Cy7 anti-mouse PD1	BioLegend	135223

BV421 anti-mouse CD44	BioLegend	103039
BV650 anti-mouse CD138	BioLegend	142518
FITC anti-mouse SiglecH	Invitrogen	11-0333-82
Goat anti-Mouse IgG (H+L)	Abcam	ab31430
Goat Anti-Mouse IgG1	Abcam	ab97240
Goat Anti-Mouse IgG2	Abcam	ab97255
Goat Anti-Mouse IgA	Abcam	ab97235

**Table S4. Primer and probe sequences used in qPCR.**

<b>Primers</b>	<b>Sequence (5'→3')</b>
COVID-19 N-F	GGGGAAGTTCTCCTGCTAGAAT
COVID-19 N-R	CAGACATTTTGCTCTCAAGCTG
COVID-19 N-Probe	FAM-TTGCTGCTGCTTGACAGATT-BHQ1
COVID-19 sgE-F	CGATCTCTTGTAGATCTGTTCTC
COVID-19 sgE-R	ATATTGCATTGCAGCAGTACGCACA
COVID-19 sgE-Probe	FAM-ACACTAGCCATCCTTACTGCGCTTCG-BHQ1